

Direct Evidence of the Anisotropic Structure of Vortices Interacting with Columnar Defects in High-Temperature Superconductors through the Analysis of Lorentz Images

Osamu KAMIMURA^{1,8*}, Hiroto KASAI^{1,8†}, Tetsuya AKASHI^{2,8‡}, Tsuyoshi MATSUDA^{1,8†}, Ken HARADA^{1,8†},
Jun MASUKO^{3‡}, Takaho YOSHIDA^{1,8}, Nobuyuki OSAKABE^{1,3}, Akira TONOMURA^{1,8†}, Marco BELEGGIA^{4§},
Giulio POZZI⁴, Jun-ichi SHIMOYAMA^{5,8}, Kohji KISHIO^{5,8}, Tetsuo HANAGURI^{5,6,8}, Koichi KITAZAWA^{5,6,8},
Masato SASASE⁷ and Satoru OKAYASU⁷

¹Advanced Research Laboratory, Hitachi, Ltd., Hatoyama, Saitama 350-0395

²Hitachi Instruments Service Co., Ltd., 4-28-8 Yotsuya, Shinjuku-ku, Tokyo 160-0004

³Department of Physics, Tokyo Institute of Technology, Ohokayama, Meguro-ku, Tokyo 152-8551

⁴Department of Physics and Istituto Nazionale per la Fisica della Materia,
University of Bologna, Viale B. Pichat 6/2, 40127 Bologna, Italy

⁵Department of Applied Chemistry, University of Tokyo, Tokyo 113-8656

⁶Department of Advanced Materials Science, School of Frontier Sciences, University of Tokyo, Tokyo 113-0033

⁷Department of Material Science, Japan Atomic Energy Research Institute, Tokai, Naka-gun, Ibaraki 319-1195

⁸SORST, Japan Science and Technology Corporation (JST), Nihonbashi, Chuo-ku, Tokyo 103-0027

(Received February 8, 2002)

Two types of Fresnel contrasts of superconducting vortices in a Lorentz micrograph, corresponding to pinned and unpinned vortices, were obtained by a newly developed 1 MV field-emission transmission electron microscope on a $\text{Bi}_2\text{Sr}_2\text{CaCu}_2\text{O}_{8+\delta}$ (Bi-2212) thin specimen containing tilted linear columnar defects introduced by heavy ion irradiation. The main features of the Fresnel contrasts could be consistently interpreted by assuming that the vortices are pinned along the tilted columnar defects and by using a layered or an anisotropic model to calculate the phase shift of the electron wave. The confirmed validity of both models strongly indicates that superconducting vortices in high-critical temperature (high- T_c) layered materials have an anisotropic structure.

KEYWORDS: superconductor, anisotropy, layered structure, superconducting vortex, columnar defect, Lorentz microscopy, electron microscopy

DOI: 10.1143/JPSJ.71.1840

Superconductors can be used as dissipation-free electrical conductors only when their vortices (magnetic flux lines) are pinned, despite the current-induced force acting on them. In high-critical temperature (high- T_c) superconductors, in which vortices can move very easily,¹⁾ the columnar defects produced by heavy-ion irradiation have been considered to be effective pinning traps, because the linear structure of the defects fits the vortex-line shape in the materials. Therefore when the vortex lines and columns are aligned in the same direction, the pinning force acting on the vortices is expected to be optimal.²⁾

The characterization of vortex lines trapped at columnar defects has been the subject of numerous studies using various techniques, for example scanning tunneling microscopy for NbSe_2 ³⁾ and the Bitter decoration method for $\text{Bi}_2\text{Sr}_2\text{CaCu}_2\text{O}_{8+\delta}$ (Bi-2212).⁴⁾ Information about the vortex lines inside a material has been inferred by measuring the macroscopic averages of pinning forces^{2,5)} and microwave magnetoabsorption,⁶⁾ and by obtaining the microscopic positions of the vortices by two-sided Bitter decoration.⁷⁾ There are, however, no methods for obtaining information about whether each vortex inside a material is actually trapped along columnar defects or not.

Lorentz microscopy^{8,9)} and electron holography¹⁰⁾ are the only methods for observing individual vortices and defects inside superconducting thin films at present. Recently, a newly developed 1 MV field-emission electron microscope¹¹⁾ allowed us to observe vortices with high contrast in Bi-2212 films thicker than 400 nm and also to obtain direct information about them inside the materials. In our previous work,¹²⁾ in Bi-2212 with columnar defects, two types of vortices were observed: one was usual and the other elongated with low contrast. The comparison between an ordinary electron micrograph and a defocused Lorentz micrograph has shown that the columnar defects are at the exact centers of elongated vortex images, indicating that they represent vortex lines trapped along tilted columnar defects. However, the predictions made on the basis of the usual flux-tube model¹³⁾ were contrary to the experimental results. In the present study, we performed a more detailed analysis of the Lorentz images in order to interpret this puzzling feature. We investigated a through-focus series of micrographs, that shows the existence of an optimal defocus, where both pinned and unpinned vortices can be detected and distinguished. We interpreted the unexpected low contrast of the pinned vortices by taking into account in the theoretical model the layered and strongly anisotropic structure of the vortices in high- T_c materials.

Single-crystal Bi-2212 was grown by the floating zone technique and was post-annealed to a slightly overdoped oxygen content ($T_c \simeq 85$ K). Columnar defects about 10 nm in diameter with a low density (0.05 column/ μm^2) were

*Central Research Laboratory, Hitachi, Ltd., Kokubunji, Tokyo 185-860.

†RIKEN, Frontier Research System, (Laboratory in Hitachi ARL, Hatoyama, Saitama 350-0395).

‡Advanced Research Laboratory, Hitachi, Ltd., Hatoyama, Saitama 350-0395.

§Department of Materials Science, Brookhaven National Laboratory, Upton, N.Y. 11973, U.S.A.

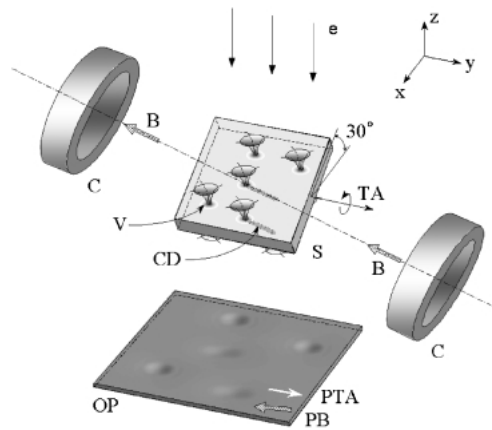


Fig. 1. Scheme of the experimental setup. e: electron beam; S: specimen; V: vortex; CD: columnar defect; TA: tilt axis; C: coils generating a magnetic field (B) in the same direction as the columnar defects. The observation plane (OP) is also shown, where contrast is generated at the vortex positions by the Fresnel phase-contrast method. Projected direction of magnetic field (PB) and projected tilt axis (PTA) onto OP are indicated by arrows.

obliquely produced at 20° with respect to the specimen surface by irradiation of 240 MeV Au^{15+} ions by using the Tandem Accelerator at the Japan Atomic Energy Research Institute (JAERI).

The experimental setup is shown in Fig. 1. A collimated electron beam (e) illuminated the specimen (S) tilted at 30° . The specimen was mounted such that the columnar defects (CD) were as parallel as possible to the tilt axis (TA), in order to detect the difference between vortex lines (V) pinned along the columnar defects and unpinned ones. The magnetic field (B), generated by the coils (C), was oriented parallel to the columnar defects. The interaction between the electron wave and the magnetic field of the vortices resulted in a phase shift of the wave, which was transformed into an intensity distribution in the observation plane (OP) by image defocusing.¹³⁾

For Bi-2212 with columnar defects, two types of vortex images have been observed in Lorentz micrographs taken at appropriate defocusing, which appeared as bright-dark globules: one with high contrast and the other with low contrast and slightly elongated in the direction of the projected tilt axis (PTA). A typical Lorentz micrograph at 30 K and 0.5 mT is shown in Fig. 2. The vortices having low contrast are indicated by arrowheads. We have confirmed that low-contrast images correspond to vortices pinned at the columnar defects, whereas high-contrast images correspond to unpinned vortices, whose direction is perpendicular to the specimen surfaces.¹²⁾ Detailed features of pinned and unpinned vortices are shown in the lower insets, revealing the contrast at selected pinned (a) and unpinned (a') vortices rendered with discrete intensity levels, so that not only the image contrast and elongation but also some image rotation of the two types of vortices can be distinguished. The image rotation described here means that the lines dividing the bright and dark regions of the vortex images are rotated.

We have noticed phenomenologically that the defocus of the microscope plays a crucial role in the image contrast and features of the vortices. Figure 3 shows a wide-range through-focus series taken at decreasing values of defocus in

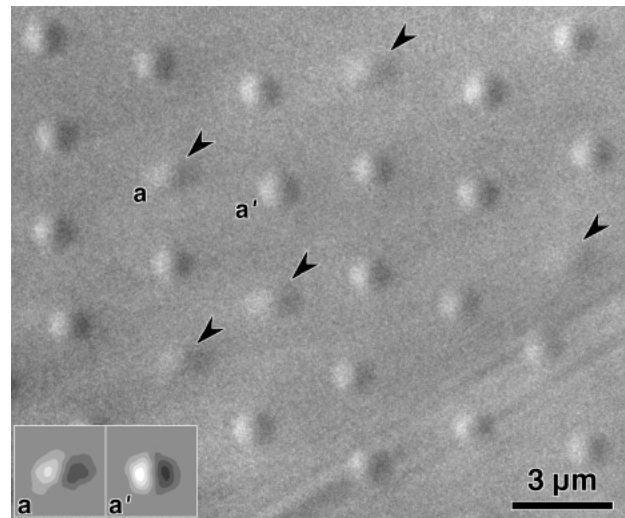


Fig. 2. Typical Lorentz micrograph taken at an appropriate defocus of 540 mm (30 K, 0.5 mT). In the lower inset, the image rotation effect at pinned (a) and unpinned (a') vortices is emphasized by discretization of the intensity levels.

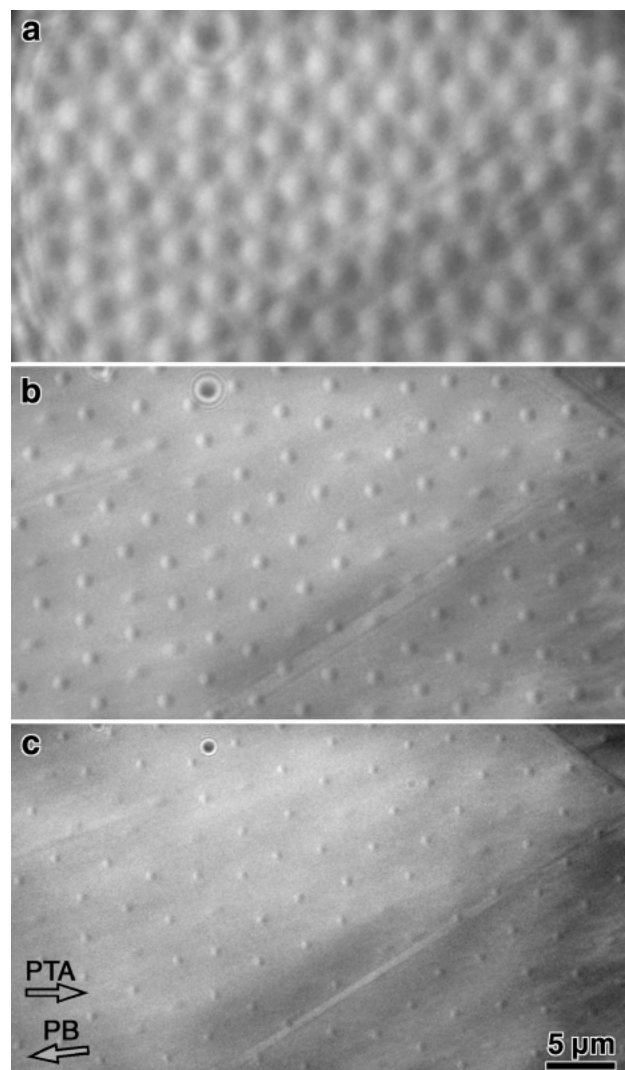


Fig. 3. Through-focus series of Lorentz micrographs at 30 K and 0.5 mT. Defocus distances were (a) 2900 mm, (b) 540 mm and (c) 230 mm. PTA and PB are also indicated by arrows.

the same specimen region. The specimen was cooled to 30 K within a magnetic field of 0.5 mT in order to avoid the effect of intrinsic pinning at low temperature.¹²⁾ At a defocus of 2900 mm, Fig. 3(a), all the vortices had the same appearance of bright-dark globules, i.e. the vortex contrast was independent of the vortex direction inside the specimen (inclined or perpendicular). The line dividing the bright and dark regions is roughly aligned perpendicular to PTA. However, decreasing the defocus to 540 mm, as in Fig. 3(b), revealed changes in contrast and shape in the image, and the vortices can be roughly divided into two types: ones with high and ones with low contrast, as is shown in Fig. 2. This difference becomes even more evident at a smaller defocus of 230 mm shown in Fig. 3(c), where the low contrast is even weaker and the vortices are sometimes difficult to detect. The through-focus observations clarified that it is necessary to select an appropriate defocus to distinguish the two types of vortices.

In order to interpret the image difference between these two types of contrast features of the vortices, we performed image simulation using the flux-tube model,¹⁴⁾ which has successfully explained the image contrast of vortices in niobium crystals. In the model, the pinned vortices are along the columnar defect whose geometry is shown in Fig. 1. The calculated results for pinned and unpinned vortices, whose parameters were specimen thickness t of 400 nm, vortex radius of 280 nm (this is a phenomenological value to account for the effect of the finite specimen thickness¹⁵⁾), and defocus of 540 mm at 1 MV accelerating voltage, are shown in Figs. 4(a) and 4(b), respectively. Although the discrepancy of the calculated figures can be understood from the increased projected length of the core,¹⁴⁾ the images in Figs. 4(a) and 4(b) do not explain the features of the experimental images in the inset of Fig. 2. The manifest discrepancy between theory and experiment may be due to the fact that the simulations did not take into account the anisotropic nature of high- T_c superconductors.

In order to confirm this hypothesis, we introduced two kinds of models: layered¹⁶⁾ and anisotropic models, by using the latest development in image interpretation, namely, the Fourier-space approach.^{16,17)} For the layered model, we managed to treat a layered structure with seven stacks ($n_L = 7$), which is the limit of our present computing facilities. The layers are separated by $t/(n_L - 1)$ and are characterized by penetration depth, $\Lambda = n_L \lambda_{ab}^2 / t$, where λ_{ab} is the transverse penetration depth characterizing the bulk material. The calculated images at the defocus of 540 mm using the layered structure model show that the contrast of the pinned vortex [Fig. 4(c)] is lower than that of the unpinned one [Fig. 4(d)] and in addition, image rotation and deformation are now present in Fig. 4(c). The results show much better agreement with the experimental images (Fig. 2) than those of the former model.

Apart from the relatively small number of layers, a major criticism that could be raised against this layered model is that the layers are coupled only through the magnetic field, so Josephson coupling is neglected. It is quite difficult to solve a layered structure with Josephson coupling, which is known as the Lawrence–Doniach model,¹⁸⁾ but very recently we succeeded in extending our Fourier approach to the anisotropic Ginzburg–Landau limit,¹⁸⁾ thereby solving the

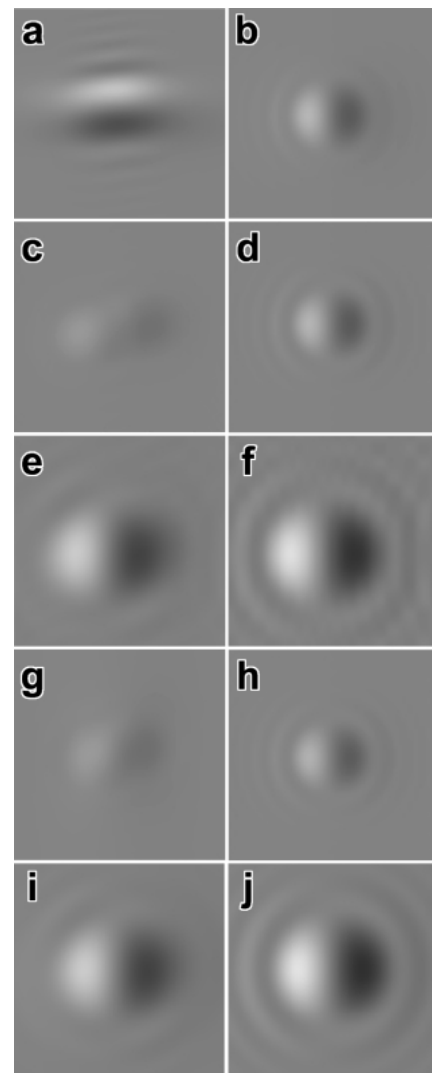


Fig. 4. Simulations of pinned (left) and unpinned (right) vortices using different models: isotropic flux-tube model [(a), (b)], layered model with seven stacks ($n_L = 7$) [(c), (d), (e), (f)] and anisotropic model with $\gamma = 200$ [(g), (h), (i), (j)]. The calculation parameters fit the experimental conditions of Figs. 2 and 3, except for the defocusing value. These were 540 mm for (a), (b), (c), (d), (g), (h) and 1300 mm for (e), (f), (i), (j).

corresponding anisotropic London equation and calculating the phase shift of the electron wave. In addition to λ_{ab} , the model introduces an additional dimensionless anisotropy parameter γ , whose value is 1 for the isotropic case and around 200 for our material. We have confirmed that in the isotropic case ($\gamma = 1$), our new model gives similar results to those in Figs. 4(a) and 4(b). The results for $\gamma = 200$ at a defocus of 540 mm are demonstrated in Figs. 4(g) and 4(h). These images also show good agreement with the experimental ones in Fig. 2, as well as with the former calculations based on the layered structure in Figs. 4(c) and 4(d).

In addition, largely defocused (1300 mm) images based on the layered model [Figs. 4(e) and 4(f)] and on the anisotropic model [Figs. 4(i) and 4(j)] are also displayed. The images of pinned and tilted vortices in Figs. 4(e) and 4(i) for both models are not deformed and have large contrast, like the unpinned vortices in Figs. 4(f) and 4(j). All these features are consistent with the experimental results.

The reason for the contrast reduction at a pinned and tilted vortex depends on many physical and experimental aspects,

for example, anisotropy factor γ , inclination of the vortex line, specimen tilt and the specimen thickness. The geometrical relationship among them is so complicated that an exact and simple interpretation is difficult, especially in the general case. However, it is possible to roughly elucidate the contrast reduction by recalling that the contrast of the vortex image recorded by Lorentz microscopy depends on the phase shift of the electron wave, which is linked to the distribution of vector potential aligned along the optical axis. That is why the specimen was mounted with a tilt of 30° (see Fig. 1): this enables the component of the vector potential parallel to the electron beam and the corresponding phase shift to give detectable effects, as shown in Fig. 4(a), where strong contrast is present when the vortex is tilted in an isotropic material. When the material is layered or has a strong anisotropic structure and the vortex line is tilted, the superconducting current along the c -axis of the crystals (Josephson current) becomes small, correspondingly reducing the component of the vector potential along the c -axis, which will no longer contribute to the total phase shift. In particular, for Bi-2212 whose γ is around 200 or for the layered model, the contribution is negligible.

This effect of contrast reduction can be confirmed more clearly by the following flat-on setup observation, where the specimen is perpendicular to the electron beam and hence has its c -axis aligned along the optical axis. If anisotropy is not taken into consideration, the effect of the superconducting current running around the vortex line produces a non-negligible component of the vector potential, and therefore non-zero contrast will be observed in the simulations. However, in this setup with the anisotropic case, the layered model gives exactly zero contrast and the isotropic model gives negligible contrast. In our experiment with this flat-on setup, we did not observe any vortex contrast for either pinned or unpinned vortices in any defocusing conditions. In other words, the flat-on experiment confirmed the existence and influence of anisotropy in the materials, and Lorentz microscopy succeeded in observing the anisotropic nature through vortex contrast, which was reduced and elongated. Although the results of both simulations (anisotropic and layered model) convincingly point out the anisotropic nature of the vortex lines, it is not yet possible to reliably extract a value for the anisotropy parameter γ .

In conclusion, not only did the experimental Lorentz

images clearly show that it is possible to distinguish vortices pinned at columnar defects from unpinned vortices, the analysis of the images also allowed us to conclude that the layered or anisotropic structure of the material is responsible for the reduced contrast of the pinned vortices and their image rotation and deformation. We are currently trying to confirm these results by conducting a more extensive comparison between experimental and simulated images.

The authors are grateful to Drs. J. Endo, T. Matsumoto, T. Onogi, R. Sugano and T. Kawasaki of Hitachi, Ltd. for their valuable discussions. Thanks are also due to Messrs. S. Saitou, S. Matsunami and N. Moriya of Hitachi, Ltd. for their technical assistance in the experiments.

- 1) G. W. Crabtree and D. R. Nelson: *Phys. Today* **50** (April, 1997) 38.
- 2) L. Civale, A. D. Marwick, T. K. Worthington, M. A. Kirk, J. R. Thompson, L. Krusin-Elbaum, Y. Sun, J. R. Clem and F. Holtzberg: *Phys. Rev. Lett.* **67** (1991) 648.
- 3) S. Behler, S. H. Pan, P. Jess, A. Baratoff, H.-J. Guntherodt, F. Levy, G. Wirth and J. Wiesner: *Phys. Rev. Lett.* **72** (1994) 1750.
- 4) H. Dai, S. Yoon, J. Liu, R. C. Budhani and C. M. Lieber: *Science* **265** (1994) 1552.
- 5) V. Hardy, A. Wahl, S. Hebert, A. Ruyter, J. Provost, D. Groult and Ch. Simon: *Phys. Rev. B* **54** (1996) 656.
- 6) T. Hanaguri, Y. Tsuchiya, S. Sakamoto and A. Maeda: *Phys. Rev. Lett.* **78** (1997) 3177.
- 7) Z. Yao, S. Yoon, H. Dai, S. Fan and C. M. Lieber: *Nature* **371** (1994) 777.
- 8) K. Harada, T. Matsuda, J. E. Bonevich, M. Igarashi, S. Kondo, G. Pozzi, U. Kawabe and A. Tonomura: *Nature* **360** (1992) 51.
- 9) K. Harada, H. Kasai, O. Kamimura, T. Matsuda, A. Tonomura, S. Okayasu and Y. Kazumata: *Phys. Rev. B* **53** (1996) 9400.
- 10) A. Tonomura: *Electron Holography* (Springer, Heidelberg, 1999) 2nd ed.
- 11) T. Kawasaki, T. Yoshida, T. Matsuda, N. Osakabe, A. Tonomura, I. Matsui and K. Kitazawa: *Appl. Phys. Lett.* **76** (2000) 1342.
- 12) A. Tonomura, H. Kasai, O. Kamimura, T. Matsuda, K. Harada, Y. Nakayama, J. Shimoyama, K. Kishio, T. Hanaguri, K. Kitazawa, M. Sasase and S. Okayasu: *Nature* **412** (2001) 620.
- 13) J. E. Bonevich, K. Harada, H. Kasai, T. Matsuda, T. Yoshida, G. Pozzi and A. Tonomura: *Phys. Rev. B* **49** (1994) 6800.
- 14) S. Fanesi, G. Pozzi, J. E. Bonevich, O. Kamimura, H. Kasai, K. Harada, T. Matsuda and A. Tonomura: *Phys. Rev. B* **59** (1999) 1426.
- 15) R. Patti and G. Pozzi: *Ultramicroscopy* **77** (1999) 163.
- 16) M. Beleggia and G. Pozzi: *Ultramicroscopy* **84** (2000) 171.
- 17) M. Beleggia and G. Pozzi: *Phys. Rev. B* **63** (2001) 54507.
- 18) M. Tinkham: *Introduction to Superconductivity* (McGraw-Hill, New York, 1996) 2nd ed.